CHAPTER - 4

DIGITAL COMPUTER SIMULATION

4.1 SPECIFICATIONS OF THE COMPUTER USED :

The computer used in the present investigation is an 8 bit INCONIX system 4000 control computer fitted with Z 80 CPU (Central Processing Unit). It has 59 K TPA (transient programme area) and is provided with 128 K of dynamic RAM (random access memory). It can be used with an auxilliary transportable memory in the form of 8" size floppy discs as it is provided with 2 numbers of 8" DSDD (double sided double density) soft sectored floppy disc drives and can accomodate two more such extra drives. It is also fitted with an STD Bus for five parts. It is available with 12" monochrome monitor which can display 24 lines of 80 character information on its screen at a time. Centronic printer interface is provided as well that can print 65 lines of 80 character information per page, using dot matrix. Provision for printing in various configurations is also available with the printer. The computer is provided with 91 Key ASCII (American Standard Code for Information Interchange) keyboard and is based on CPM 3 PLUS Operating System.

The software supplied with this computer includes WORDSTAR and SPELSTAR for character manipulation and text analysis. Additionally, it is provided with BASIC, FORTRAN, PASCAL, COBOL, DBASE II, ASSEMBLY and SUPERCALC compilers.

4.2 FORTRAN IV COMPUTER PROGRAM :

Based on the computational algorithm developed earlier in art.3.3 and the flow chart displayed in Appendix : A-5, a computer programme in FORTRAN IV was developed for the

present investigation. The programme uses the following sub-routines :

i) Subroutine MESH for automatically generating nodal co-ordinates and other geometric data for the finite element grid with right angled triangular elements chosen.

ii) Subroutine MODIFY to take into account effect of aspect ratio on grid geometry.

iii) Subroutine PHI1F which generates conduction generation vector for conduction solution.

iv) Subroutine MSHOUT for printing mesh co-ordinates and element areas.

v) Subroutine BCS which provides values of the functions Ψ, θ and ω at the boundary nodes automatically for Dirichlet or Neumann boundary conditions.

vi) Subroutine SOLVE1 for solving the sets of simultaneous equations, eqns. (3.19, 3.20 and 3.21), using Gauss-Seidel method of matrix iterations.

vii) Subroutine OUTPUT for printing the results.

The main programme code in FORTRAN which uses the above subroutines is documented in Appendix : A-6.

4.3 SELECTION OF IMPORTANT PARAMETERS :

Before plunging into the main investigation, preliminary numerical experiments were performed for identifying the effects of various key parameters like boundary conditions, no.of

elements, tolerance levels etc., based on which, these parameters were selected for the present investigation. These experiments are discussed now, as under :

4.3.1 **Selection of Boundary conditions :** Boundary conditions for the top and bottom walls of the enclosure was of Dirichlet type from the problem definition, however, there was an option of selecting boundary condition for the side walls. So, a numerical experiment was performed to obtain the influence of side wall boundary condition. Fig. 4.1 represents the results of this experiment. It was observed that Dirichlet boundary condition gives higher value of gap conductance compared to that obtained using Neumann boundary condition at all gap heights and aspect ratios. However, the difference is aspect ratio dependent and reduces with increase in aspect ratio. As the present investigation concerns high aspect ratio enclosures, and as Neumann boundary condition results in reduction in no.of effective boundary nodes, culminating in increased approximation, Dirichlet boundary condition for side walls was selected for the present investigation.

4.3.2 **Selection of Number of Elements :** Fig.4.2 represents the effect of number of elements on computing time and Nusselt number while Fig.4.3 shows the same in percentage. It was observed from Fig.4.3 that increasing the number of elements from 32 to 200 resulted in 12.5% reduction in Nusselt number but increased computing time by 1130%. Close study of Fig.4.2 also reveals that the curve for both the computing time and Nu are flat near NEL=32, while the curve for computing time shoots up exponentially near NEL=200. Thus, a compromise was made between accuracy and

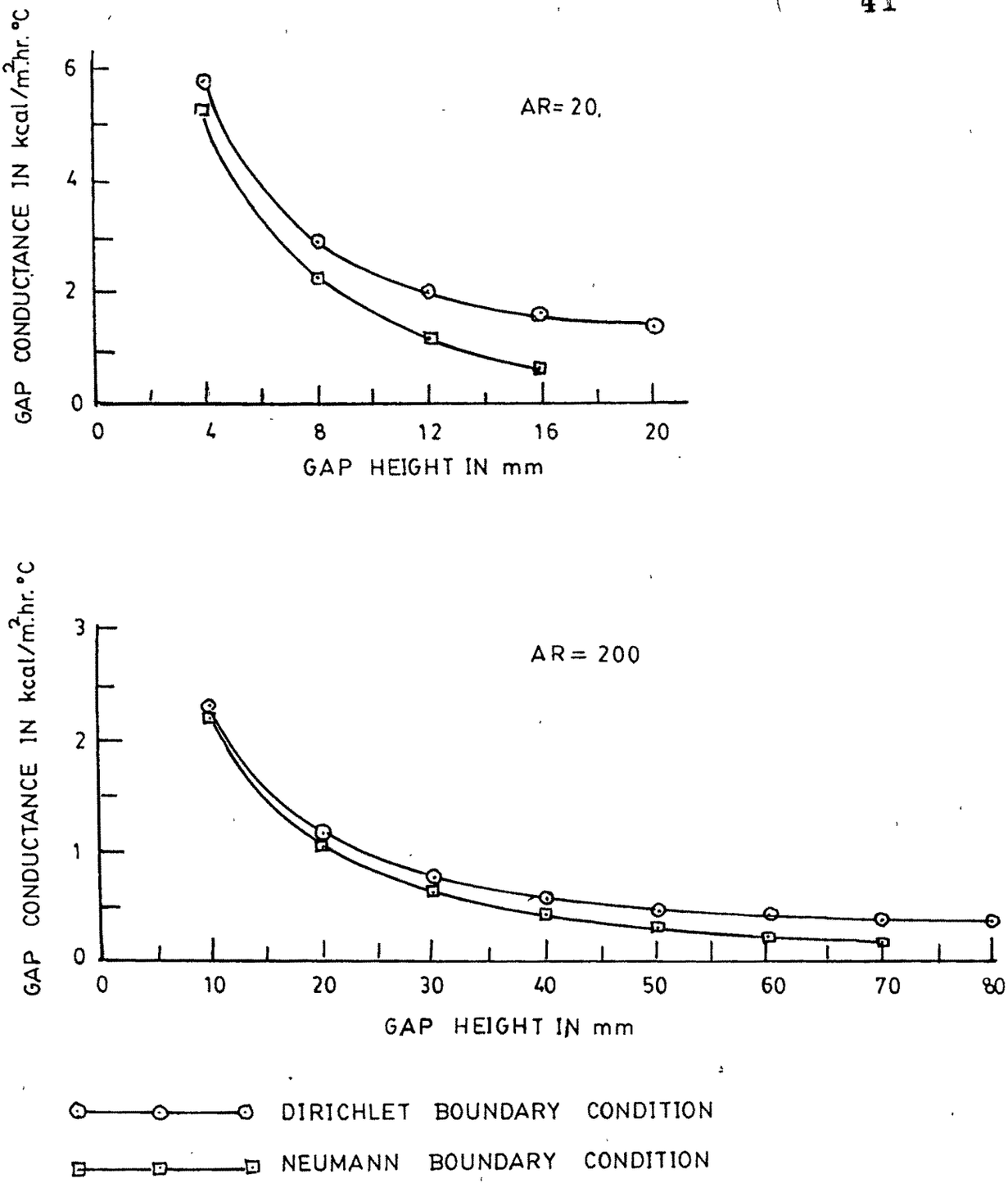
GAP CONDUCTANCE IN kcal/m².hr.°C
AR= 20,
GAP HEIGHT IN mm
AR= 200
GAP CONDUCTANCE IN kcal/m².hr.°C
GAP HEIGHT IN mm
DIRICHLET BOUNDARY CONDITION
NEUMANN BOUNDARY CONDITION

FIG: 4·1

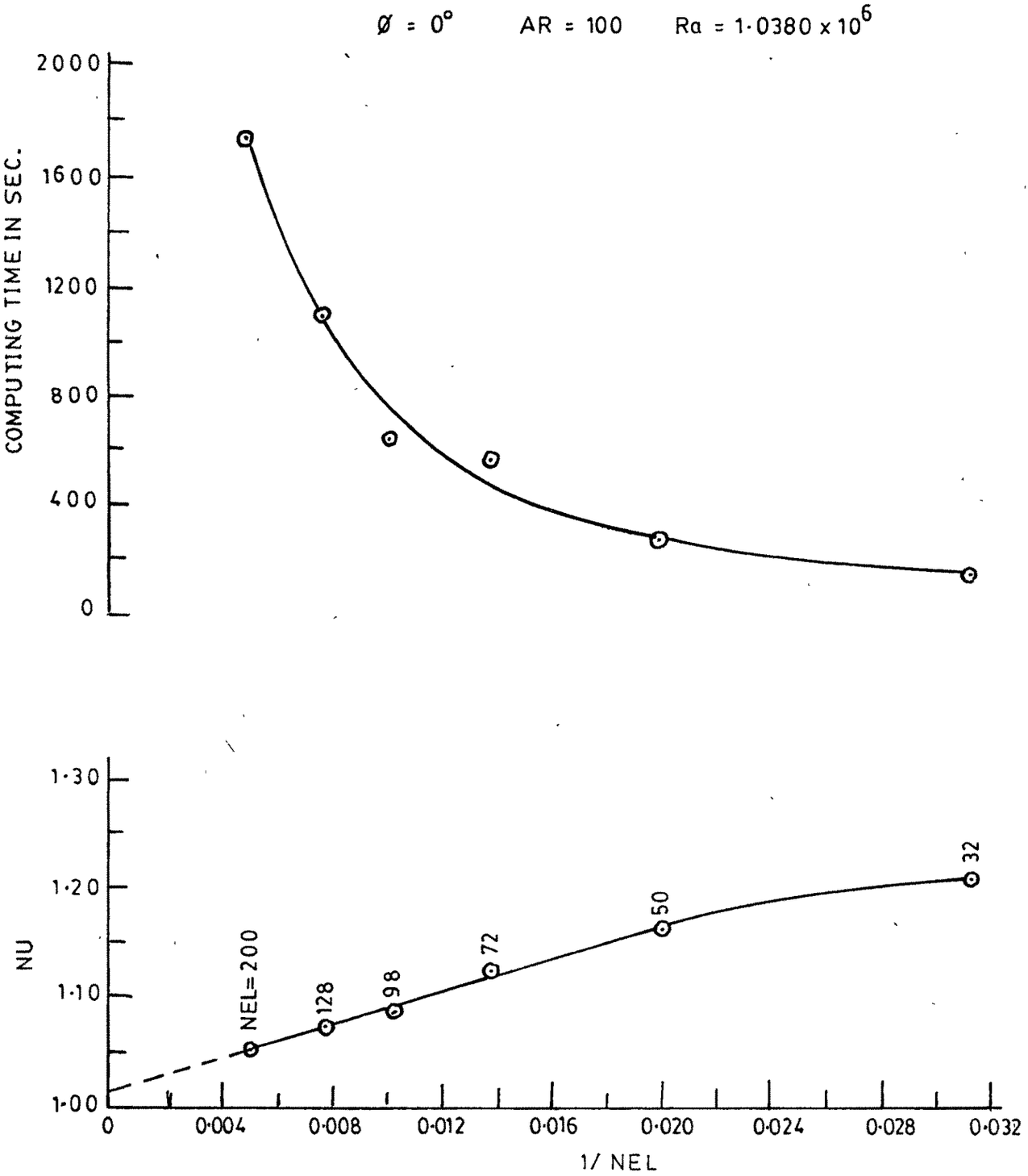
Ø = 0°
AR = 100
Ra = 1·0380 x 10^6
COMPUTING TIME IN SEC.
2000
1600
1200
800
400
0
NU
1·30
1·20
1·10
1·00
NEL= 200
128
98
72
50
32
0
0·004
0·008
0·012
0·016
0·020
0·024
0·028
0·032
1/ NEL

FIG: 4·2

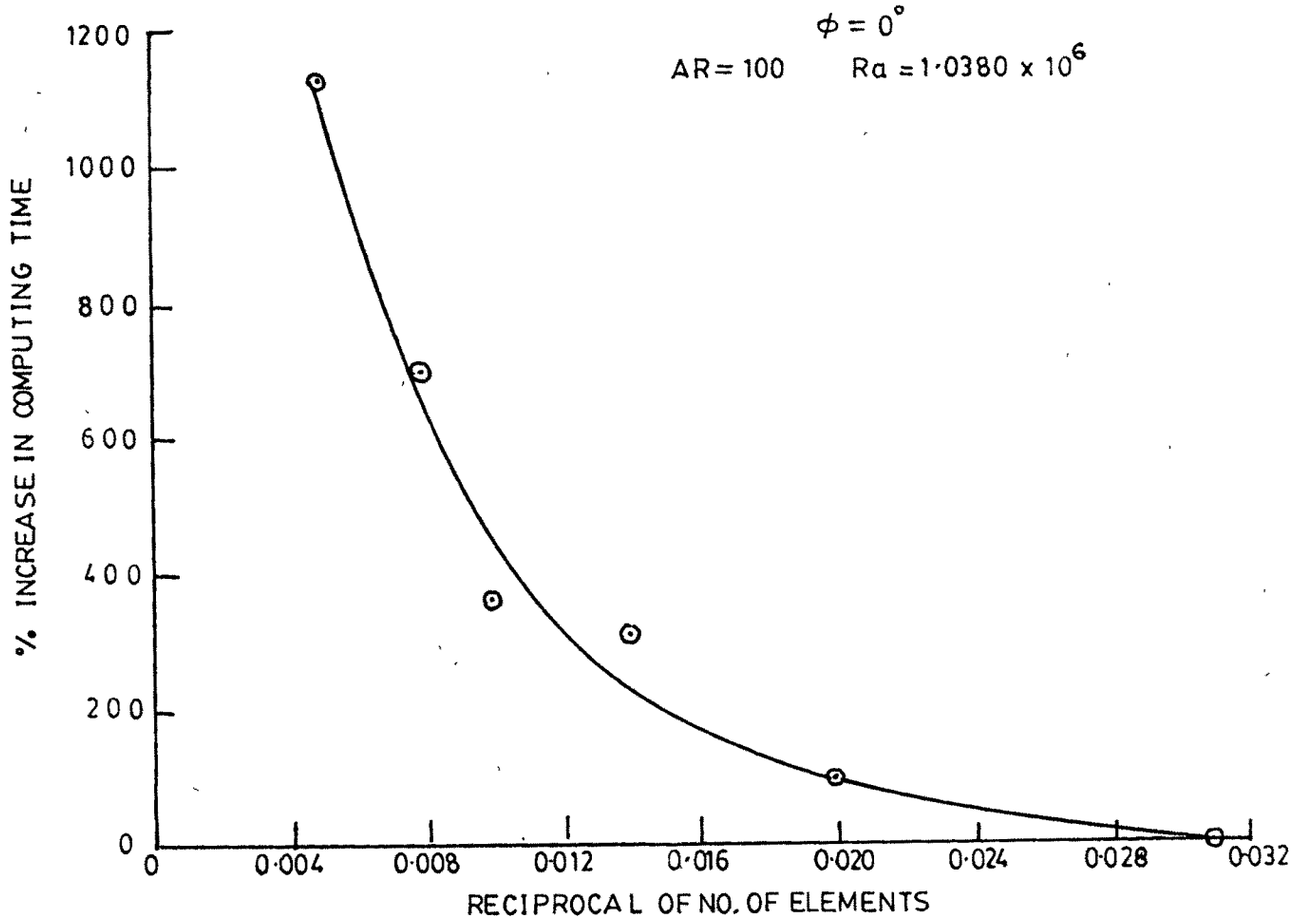
$\phi = 0^\circ$
AR = 100 Ra = 1·0380 x 10^6
% INCREASE IN COMPUTING TIME
1200
1000
800
600
400
200
0
0·004
0·008
0·012
0·016
0·020
0·024
0·028
0·032
RECIPROCAL OF NO. OF ELEMENTS

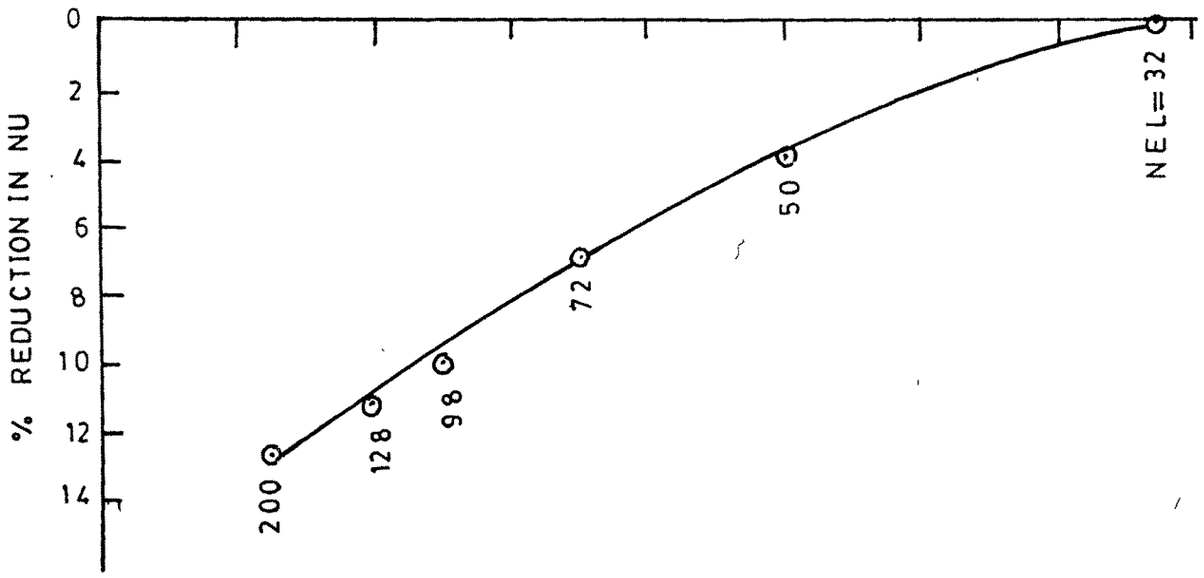
% REDUCTION IN NU
0
2
4
6
8
10
12
14
200
128
98
72
50
NEL=32

FIG: 4·3

economy of computation by selecting a finite element grid with 32 right angled - triangular elements having 25 nodes.

4.3.3 Selection of Tolerance Levels (Sensitivity Analysis) :

A sensitivity analysis was performed in order to choose relative tolerance limits or permissble error limits i.e. (new value-old value)/new value, for the system variables Ψ , θ and ω. For this, the equations were iterated indefinitely and the error values Ψ_{error}, θ_{error} and ω_{error} were documented for each iterations.

Fig.4.4, 4.5 and 4.6 represent the results of this analysis, for different aspect ratios and Rayleigh numbers. As can be observed, relative error for temperature reduces steadily and remains insensitive and very low, even when those for stream function and vorticity are relatively large containing initial bursts or fluctuations, though gradually reducing, with outer iterations. This shows that larger error limits for stream function and vorticity function can very well be tolerated by temperature function, in so far as its error limits are chosen low enough.

Thus, relative tolerance limits were fixed at 0.1 (10%) for stream function (Ψ) and vorticity function (ω) solutions and at 0.05 (5%) for temperature (θ) solution. Above criteria resulted in 2, 9 and 2 internal iterations respectively for Ψ , θ and ω solutions and about 17 outer iterations were required for overall convergence within the permissible error limits. It is interesting to note that CPU time for the above scheme was of the order of 33 minutes for each run, while a test run made with a uniform error limit

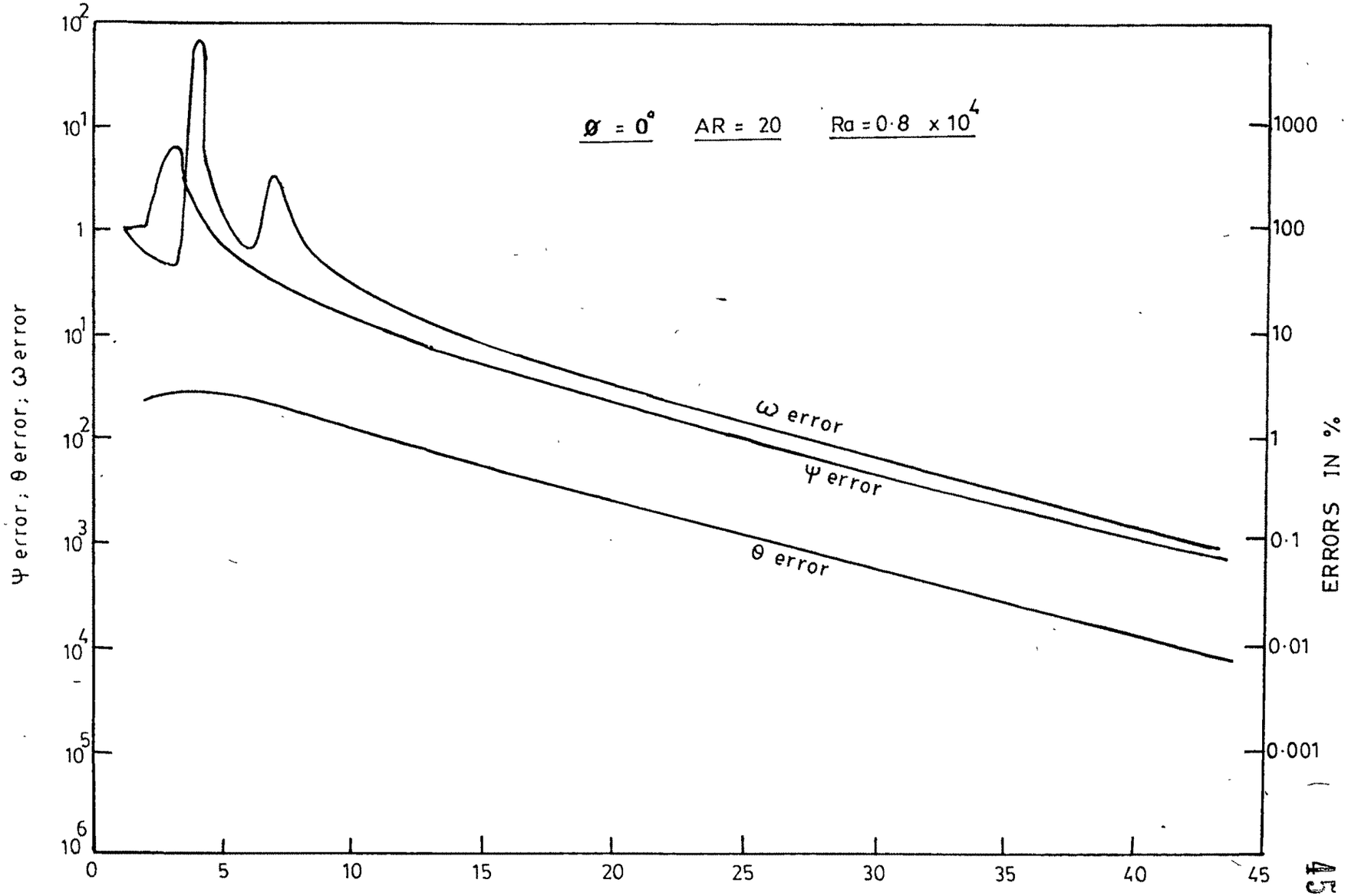
ø = 0°
AR = 20
Ra = 0·8 x 10^4
ω error
ψ error
θ error
ψ error; θ error; ω error
ERRORS IN %
NO. OF OUTER ITERATIONS
10^2
10^1
1
10^1
10^2
10^3
10^4
10^5
10^6
1000
100
10
1
0·1
0·01
0·001
0
5
10
15
20
25
30
35
40
45

FIG: 4·4

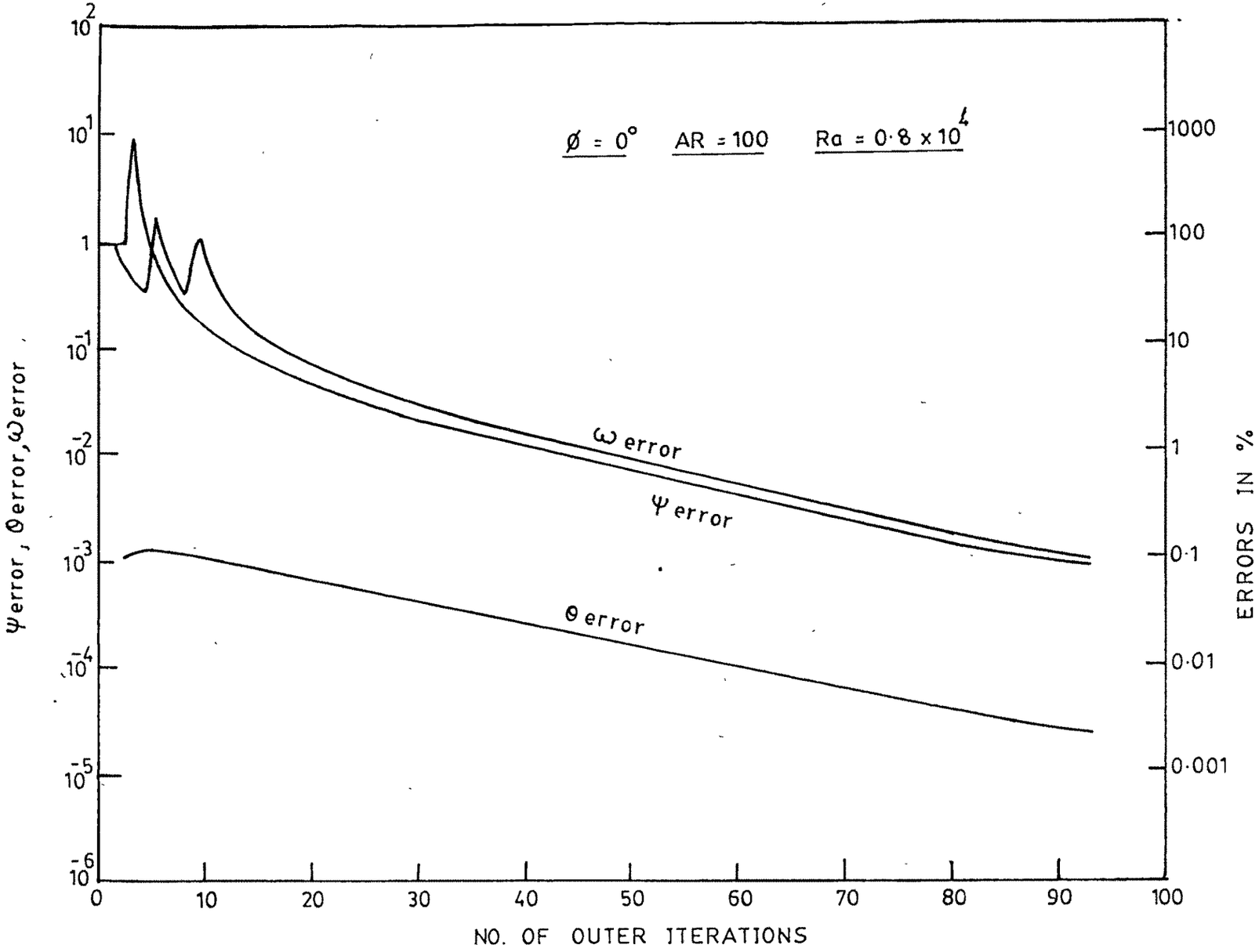
10^2
10^1
1
10^{-1}
10^{-2}
10^{-3}
10^{-4}
10^{-5}
10^{-6}
$\phi = 0°$ AR = 100 Ra = 0.8×10^4
ω error
ψ error
θ error
ψerror , θerror, ωerror
1000
100
10
1
0·1
0·01
0·001
ERRORS IN %
0
10
20
30
40
50
60
70
80
90
100
NO. OF OUTER ITERATIONS

FIG: 4·5

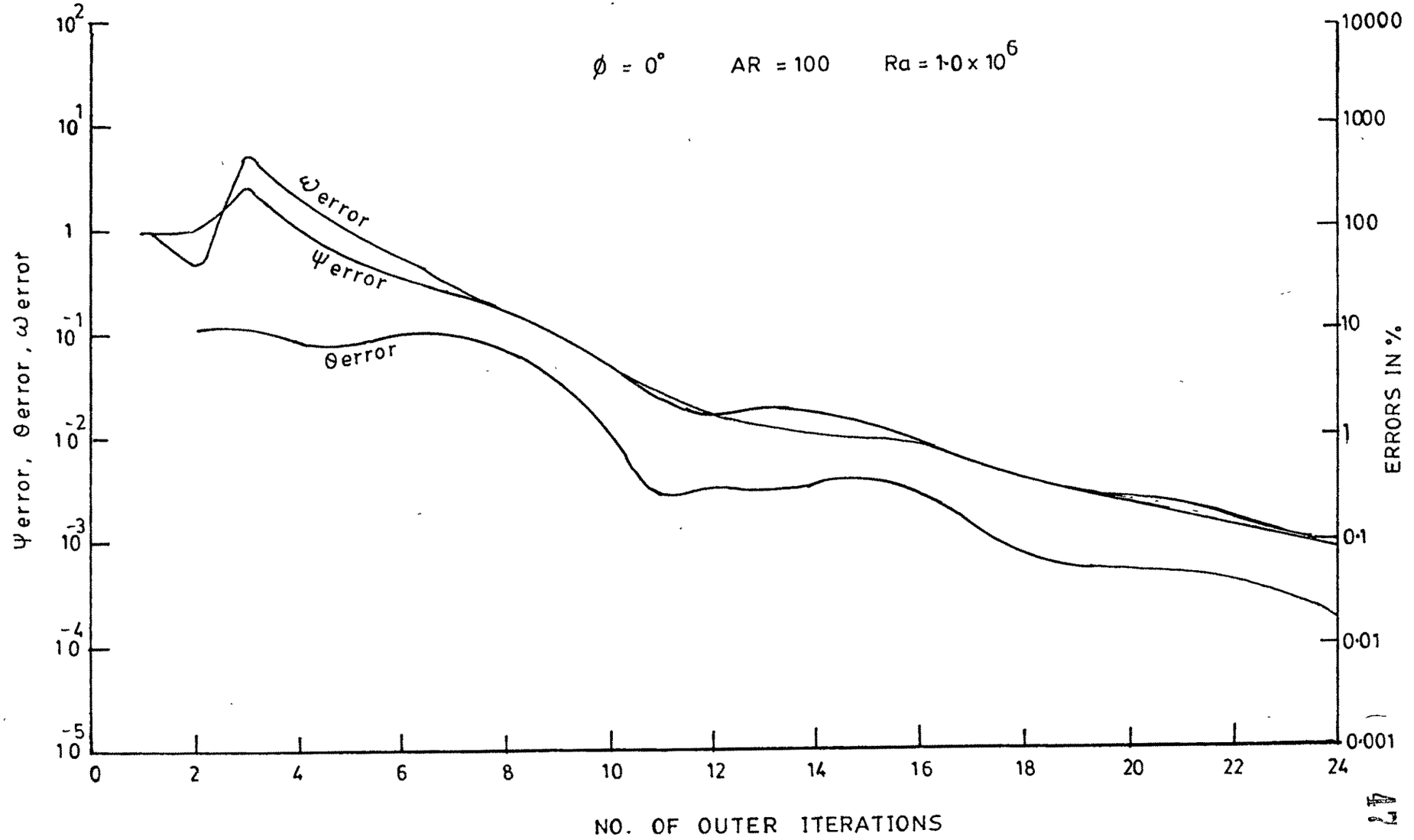
ϕ = 0° AR = 100 Ra = 1·0 x 10^6
ωerror
ψerror
θerror
ψerror, θerror, ωerror
ERRORS IN %
NO. OF OUTER ITERATIONS
10^2
10^1
1
10^{-1}
10^{-2}
10^{-3}
10^{-4}
10^{-5}
10000
1000
100
10
1
0·1
0·01
0·001
0
2
4
6
8
10
12
14
16
18
20
22
24

FIG: 4·6

of 0.01 (1%) for all the three variables required CPU time of 95 minutes, while giving results, differing by not more than 0.7%, for Nusselt number.

It may be noted that actual relative errors in temperature solutions were much below the tolerance limit of 0.05 i.e. 5%, selected in the present investigation. For example, it can be varified from Fig.4.4 that, for ω error of 10%, when the iterations terminate at the end of 14th iteration, θ error is less than 1%, well below the tolerance limit of 5%, selected for temperature.

Comparing Fig.4.4 with Fig.4.5, it was observed that for ωerror of 10%, 14 iterations were needed at AR=20, while 16 iterations were required at AR=100. Also, comparision of Fig.4.5 with Fig.4.6 reveals that, while 16 iterations were required at Ra=0.8 X 10^4, only 9 iterations were needed at Ra=1 X 10^6, for ωerror of 10%. This shows that number of outer iterations required for convergence increases with increase in aspect ratio and with decrease in Rayleigh number. Also, as the curve for ω error is top most in the above figures, it may be concluded that vorticity function is the key variable that will decide the convergence or otherwise of the solution.

Numerical experiments were performed to investigate the effect of selected tolerance on actual errors, number of iterations and Nusselt number, the results of which are exhibited in Fig.4.7, 4.8 and 4.9. A close study of these figures reveals that ωerror values are of the order of tolerance levels while θerror values are much below tolerance levels, at all tolerance

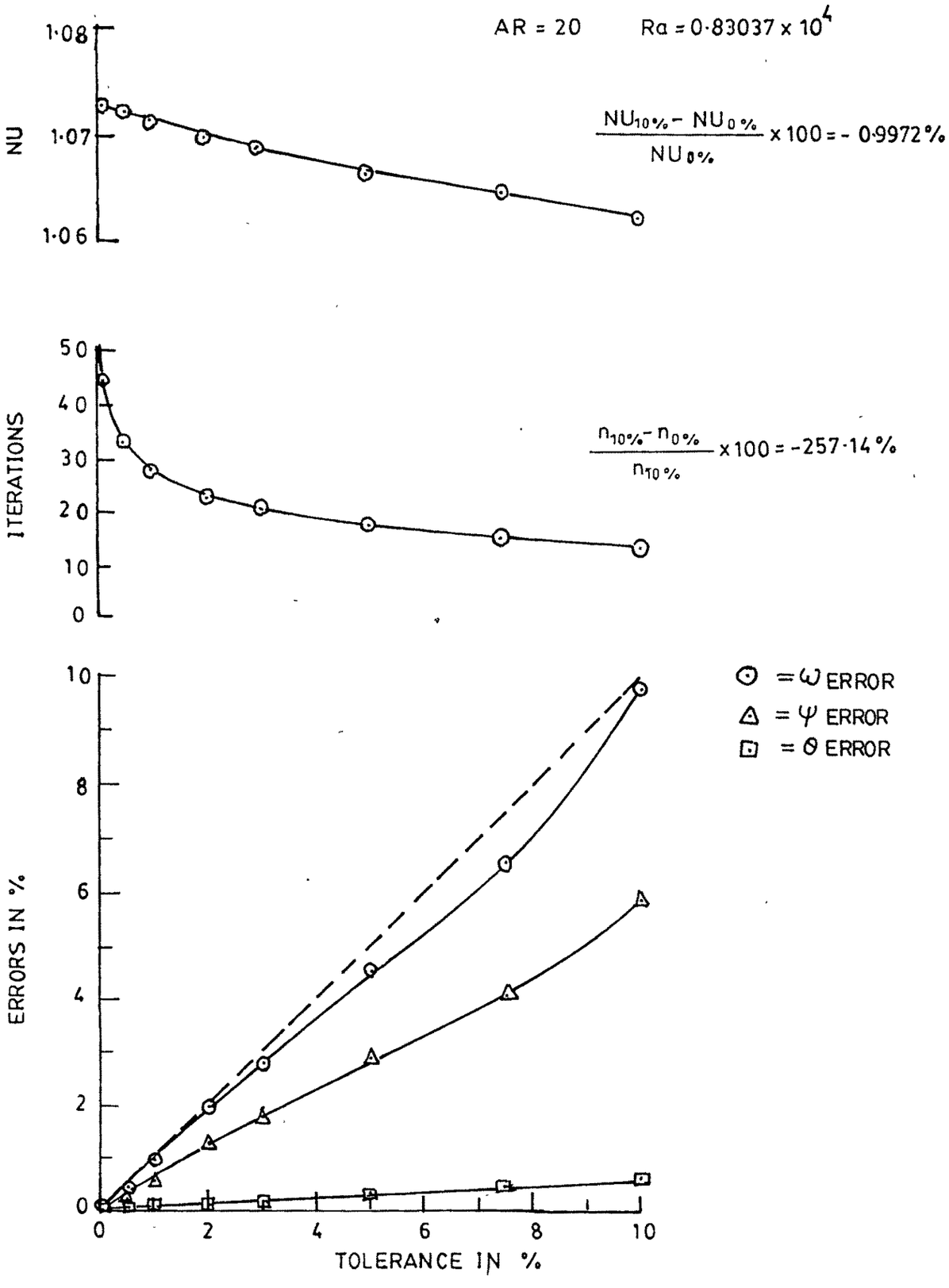
AR = 20
Ra = 0·83037 x 10^4
NU
1·08
1·07
1·06
$\frac{NU_{10\%} - NU_{0\%}}{NU_{0\%}} \times 100 = -0.9972\%$
ITERATIONS
50
40
30
20
10
0
$\frac{n_{10\%} - n_{0\%}}{n_{10\%}} \times 100 = -257.14\%$
ERRORS IN %
10
8
6
4
2
0
0
2
4
6
8
10
TOLERANCE IN %
⊙ = ω ERROR
△ = Ψ ERROR
⊡ = θ ERROR

FIG: 4·7

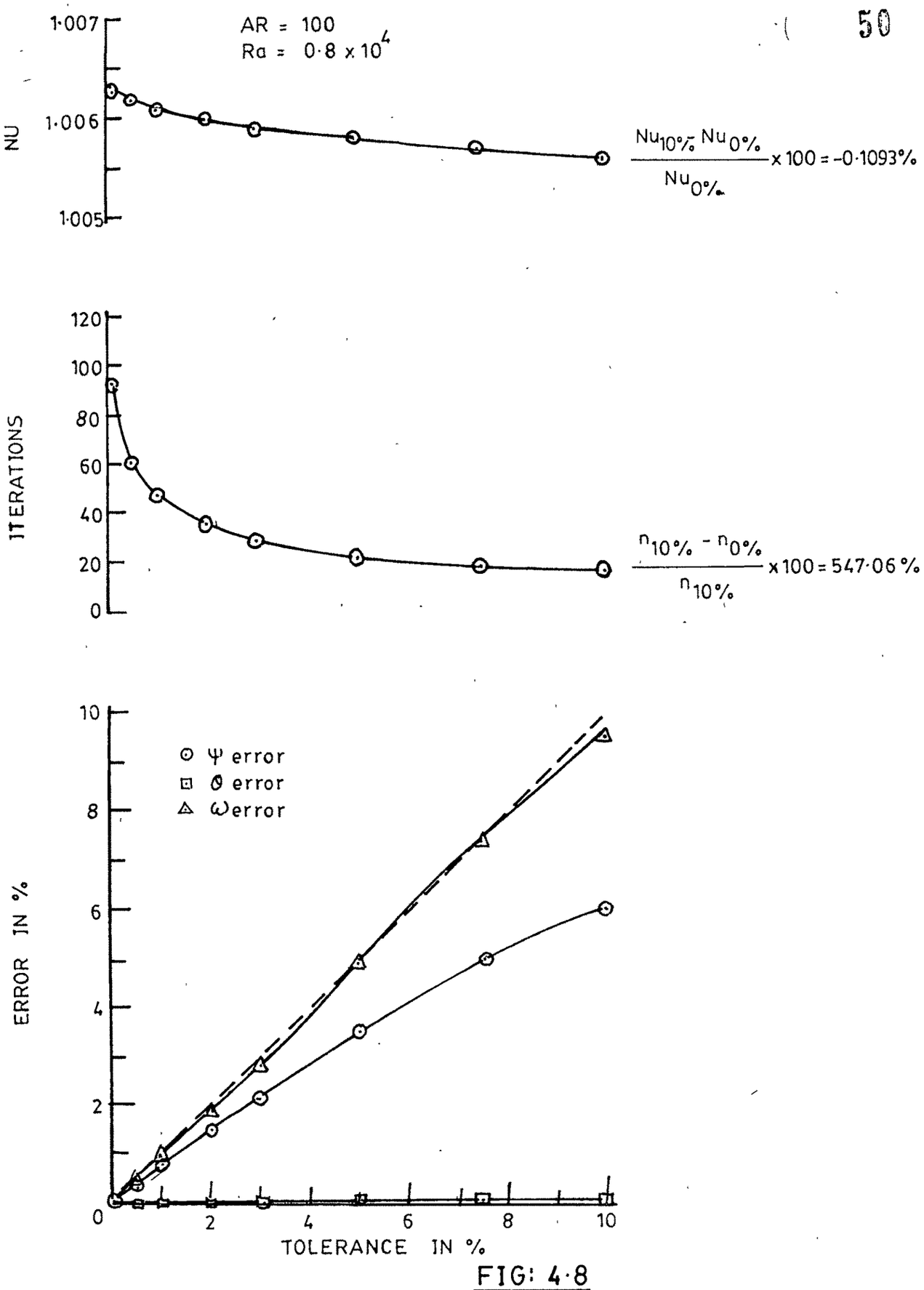
AR = 100
Ra = 0·8 x 10⁴
NU
1·007
1·006
1·005
$\frac{Nu_{10\%} - Nu_{0\%}}{Nu_{0\%}} \times 100 = -0.1093\%$
ITERATIONS
120
100
80
60
40
20
0
$\frac{n_{10\%} - n_{0\%}}{n_{10\%}} \times 100 = 547.06\%$
ERROR IN %
10
8
6
4
2
0
⊙ Ψ error
⊡ Ø error
△ ω error
2
4
6
8
10
TOLERANCE IN %

FIG: 4·8

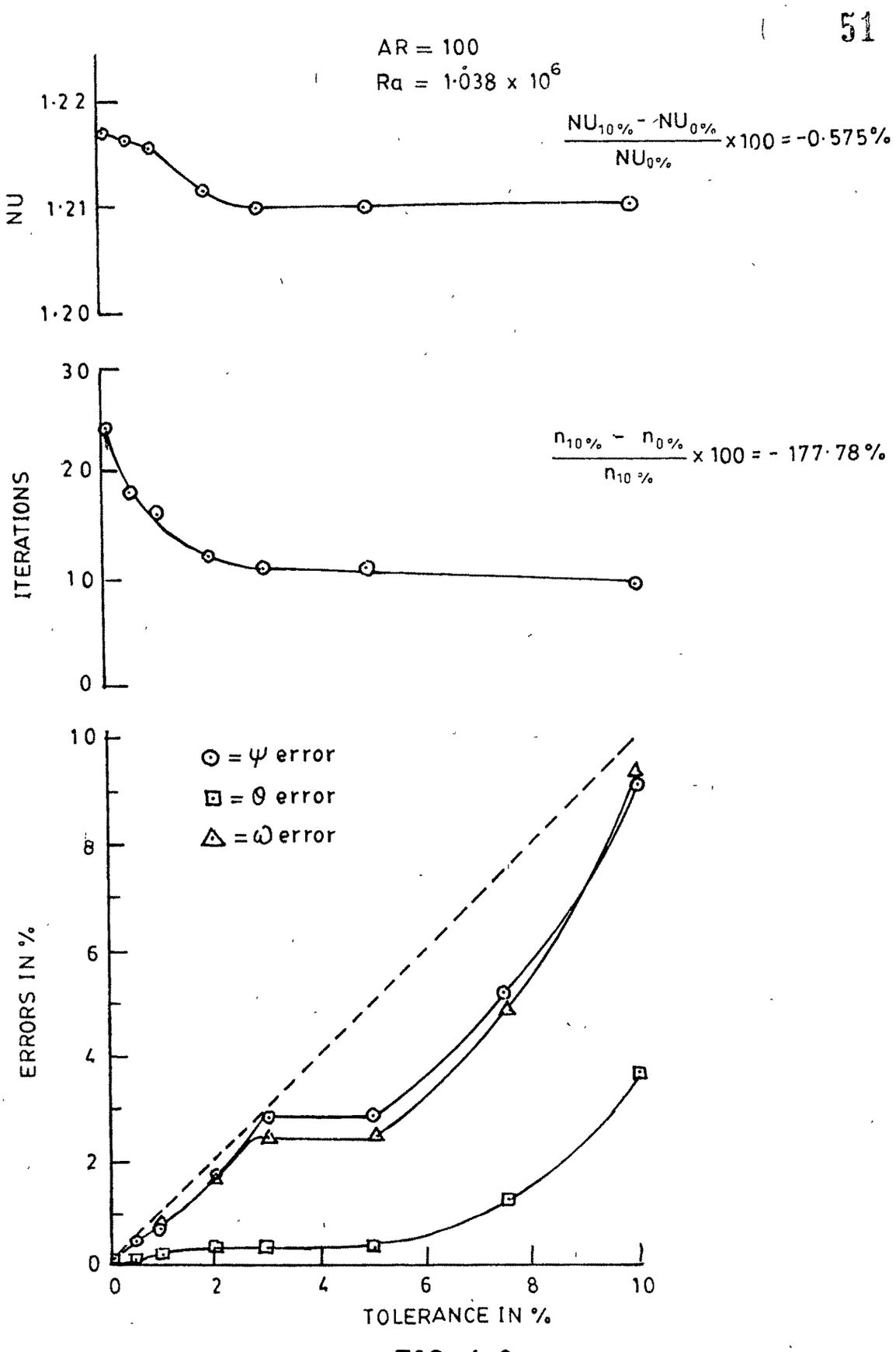
AR = 100
Ra = 1·038 x 10^6
NU
1·22
1·21
1·20
$\frac{NU_{10\%} - NU_{0\%}}{NU_{0\%}} \times 100 = -0.575\%$
ITERATIONS
30
20
10
0
$\frac{n_{10\%} - n_{0\%}}{n_{10\%}} \times 100 = -177.78\%$
ERRORS IN %
10
8
6
4
2
0
⊙ = ψ error
⊡ = θ error
△ = ω error
0
2
4
6
8
10
TOLERANCE IN %

FIG: 4·9

levels selected, for various Ra and AR values chosen as parameters. This suggests that it is the vorticity function (ω), which should be closely watched for obtaining a stable solution. Another interesting observation from the above figures is that increasing the tolerance from 0% (extrapolated ideal condition) to 10%, changes the Nusselt number by not more than 1% while at the same time reducing the number of outer iterations from anywhere between 175% to 550%. This shows that relatively liberal tolerance levels may always be selected for variables ψ, θ and ω, for economising in CPU time, practically without any loss of accuracy in the results.

Effect of Rayleigh number (Ra) and aspect ratio (AR) on θ error V/s tolerance curve and on number of outer iterations v/s tolerance curve, is shown in Fig.4.10 and Fig.4.11 respectively. Fig.4.10 reveals that θ error increases with decrease in aspect ratio for a given Ra value at all tolerance levels, though the increase is seen to be moderate. It also depicts that error increases with increase in Rayleigh number for a given AR value at all tolerance levels, however, the increase is quite considerable at higher tolerances, though quite below selected tolerance levels. This shows that we may expect θ errors exceeding their tolerance levels, if tolerance levels selected for θ are too liberal and if Ra values are high enough. In such a case, we may get an instability, which should be closely watched for.

Fig.4.11 on the other hand, represents the effect of Rayleigh number and aspect ratio on number of outer iterations required for convergence at various

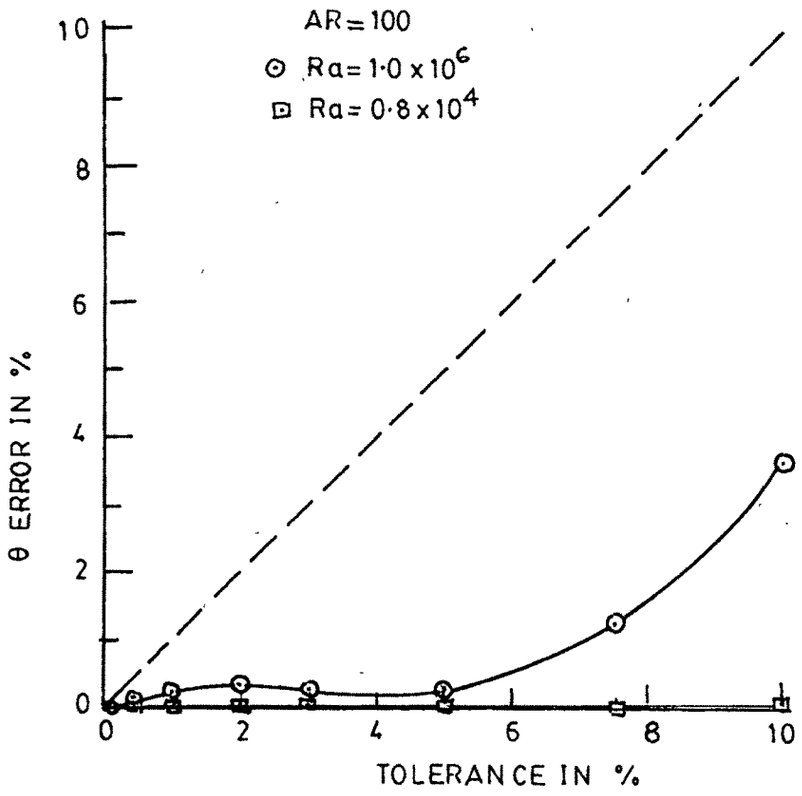
AR = 100
Ra = 1·0 x 10^6
Ra = 0·8 x 10^4
θ ERROR IN %
TOLERANCE IN %
0
2
4
6
8
10

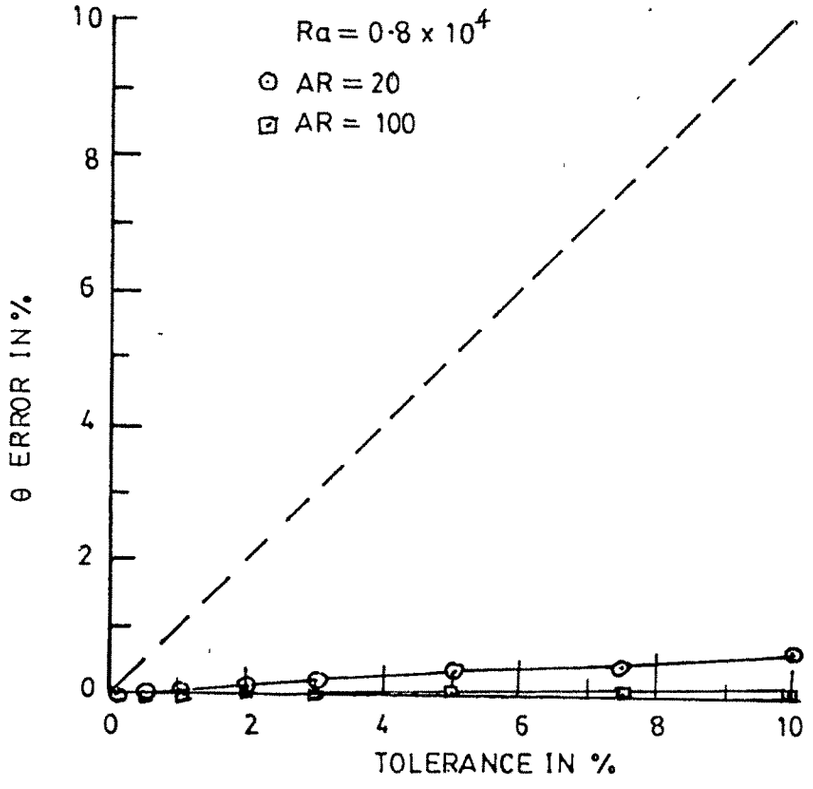
Ra = 0·8 x 10^4
AR = 20
AR = 100
θ ERROR IN %
TOLERANCE IN %
0
2
4
6
8
10

FIG: 4·10

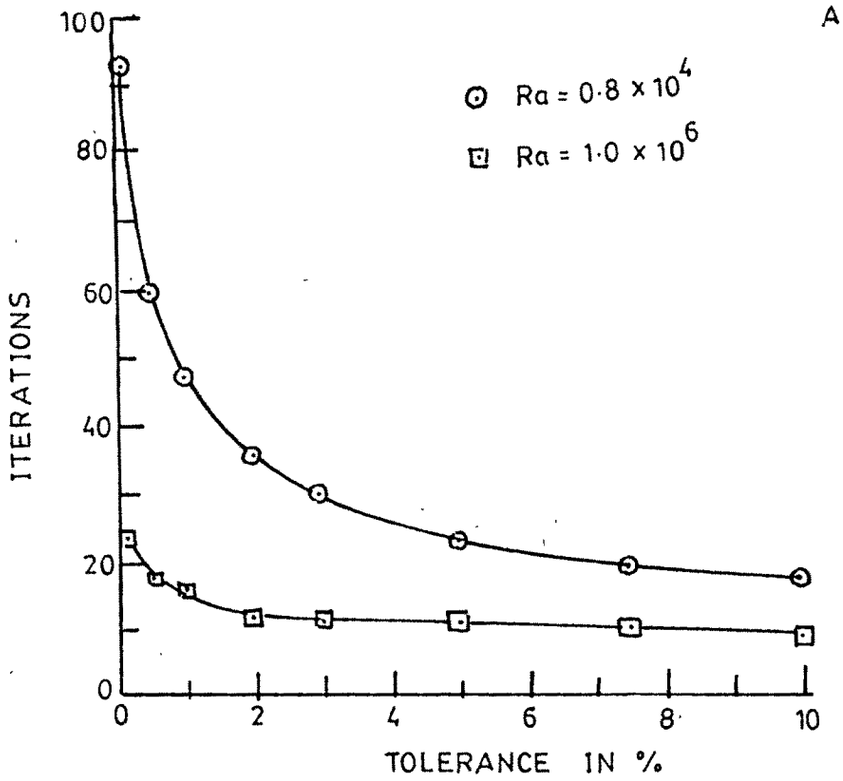
AR = 100
Ra = 0·8 x 10^4
Ra = 1·0 x 10^6
ITERATIONS
TOLERANCE IN %
0
20
40
60
80
100
0
2
4
6
8
10

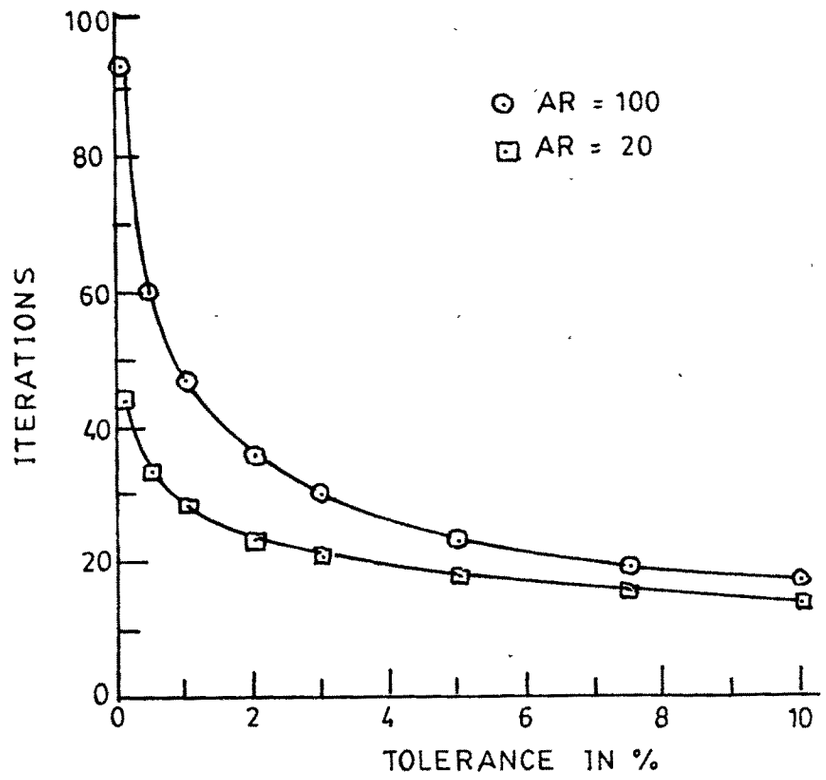
AR = 100
AR = 20
Ra = 0·8 x 10^4
ITERATIONS
TOLERANCE IN %
0
20
40
60
80
100
0
2
4
6
8
10

FIG: 4·11

tolerance levels. This shows that number of outer iterations increases with decrease in Ra values for a given aspect ratio and with increase in AR values for a given Rayleigh number, at all tolerance levels. However, this increase is more pronounced at lower tolerance levels.

We may summarise the results of the sensitivity analysis as under :

i) Larger tolerance limits can be accomodated by stream function and vorticity without impairing the accuracy of the results, in so far as the tolerance limits for temperature are chosen low enough.

ii) Larger tolerance limits for Ψ and ω and a smaller tolerance limit for θ , results in considerable saving of computing time, without significantly impairing the accuracy of the results.

iii) Actual errors in temperature solutions are far below the selected tolerance limit, though the errors in vorticity solutions are of the order of selected tolerance limit.

iv) Number of outer iterations required for convergence increases with decrease in Ra and with increase in AR.

v) Vorticity function is the variable that decides the convergence or otherwise of the solution.

vi) θ error increases with decrease in AR and with

increase in Ra at all tolerance levels.

vii) At high Ra values, errors in temperature solution may exceed its tolerance limit if they are too large, resulting into an arithmetic instability.

4.3.4 Study of Convergence and overflow conditions : Effect of aspect ratio and Rayleigh number on number of cycles for convergence to the selected tolerance level is shown in Fig.4.12. It was observed that the number of outer iterations (i.e. cycles) for convergence reduces with increase in Rayleigh number for all aspect ratios. It is interesting to note that the maximum number of cycles for convergence were 17 while minimum number of cycles for convergence were 9 at all the aspect ratios investigated. It may also be noted that, at all aspect ratios, as the Ra value exceeds that corresponding to minimum number of cycles for convergence, number of cycles for convergence shoots up almost vertically, eventually resulting in arithmetic overflow condition and solution breakdown.

The value of Ra at which such an arithmetic overflow condition appears and solution breakdown occurs, depends strongly upon aspect ratio, as can be observed from Fig.4.13. This dependence can be correlated as,

$$(Ra)_{ov} = 562.34\ AR^2 \quad \text{for} \quad 20 \leqslant AR \leqslant 300 \qquad \ldots\ldots \qquad (4.1)$$

Fig.4.14 is an extension of Fig.4.13, which includes aspect ratios from 1 to 300. An interesting point revealed in this figure is that the curve indicates the presence of three distinct regions. In the region where AR varies from 1 to 5, Ra for overflow is independent of aspect ratio while in the region where

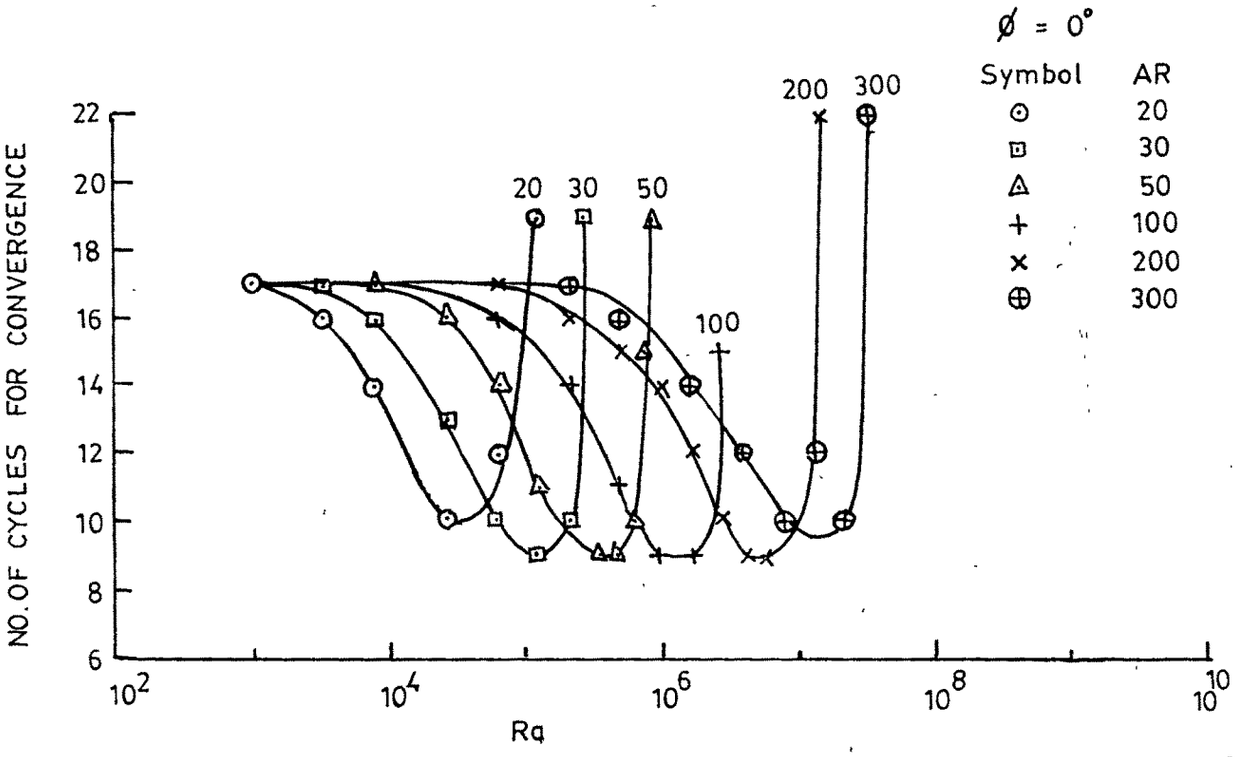

FIG: 4·12

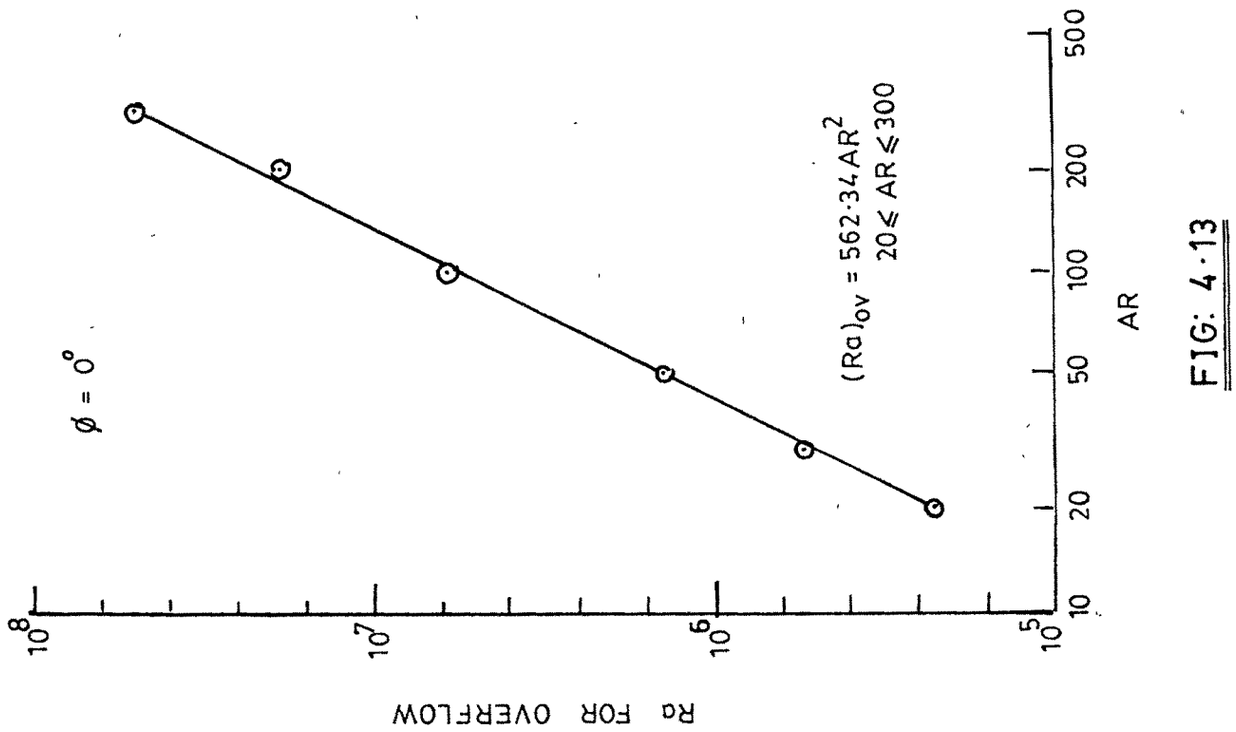

FIG: 4·13

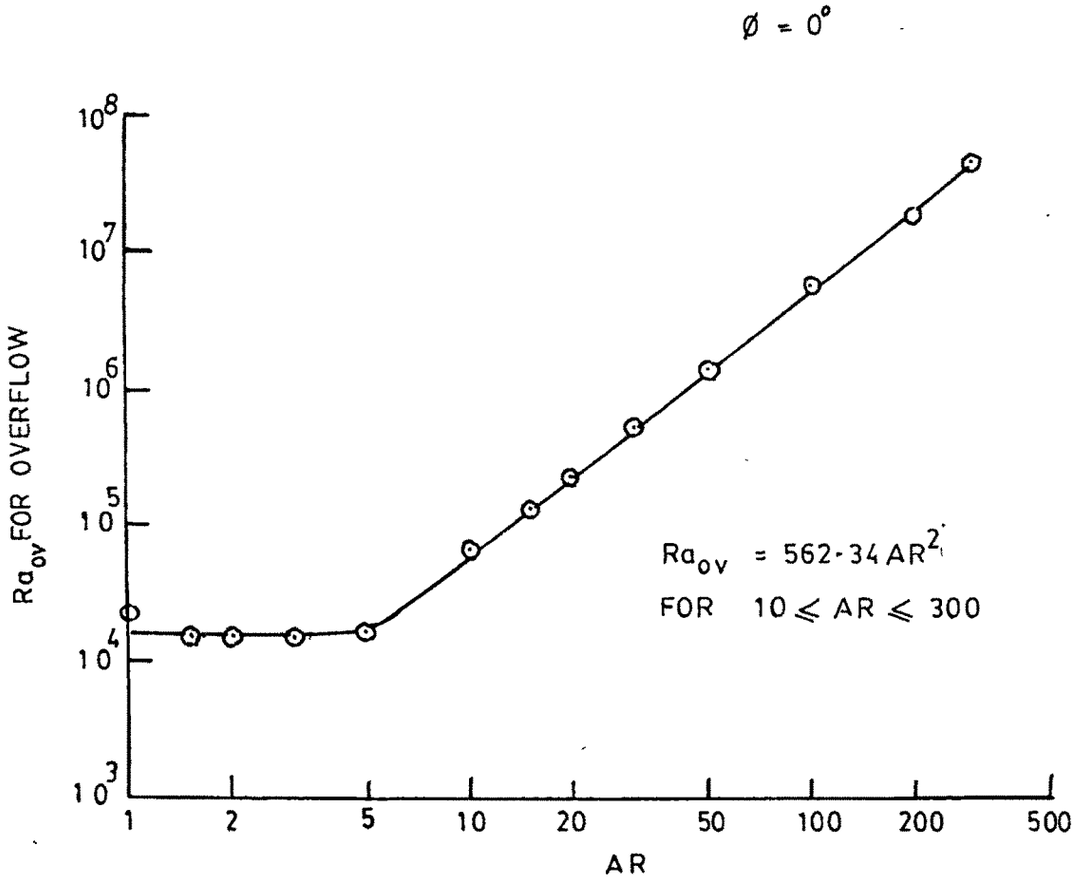
Ø = 0°
Ra_{ov} FOR OVERFLOW
10^8
10^7
10^6
10^5
10^4
10^3
$Ra_{ov} = 562{\cdot}34\,AR^2$
FOR $10 \leqslant AR \leqslant 300$
1
2
5
10
20
50
100
200
500
AR

FIG: 4·14

AR varies from 10 to 300, it varies as square of aspect ratio. The intermediate region $5 \leqslant AR \leqslant 10$, appears to be of transition type where a smooth transition from one region to another is effected.

Fig.4.15 is the result a preliminary study undertaken to investigate the effect of enclosure inclination (ϕ) with reference to horizontal, on arithmetic overflow condition. It shows that the gap height and hence Ra for overflow increases with aspect ratio at all inclinations from 0° to 180°. It also shows that Ra for overflow decreases dramatically with increase in inclination for $0° \leqslant \phi \leqslant 90°$ and with decrease in inclination for $90° \leqslant \phi \leqslant 180°$ and at $\phi = 90°$, solution breakdown occurs at a dramatically low value of gap height (2 mm) or Rayleigh number (66). This shows that the present method fails to give results for inclined enclosures, particularly near vertical orientation and a fresh approach is needed to obtain a satisfactory solution.

4.3.5 History of Central Temperature : History of central temperature for a typical enclosure from iteration to iteration for both inner and outer iterations is shown in Fig.4.16. This shows that during any outer or global iteration considered, the central temperature gradually increases with number of inner or local iterations and eventually settles down to constant value when internal or local convergence occurs. This internally converged central temperature, is again dependent upon outer iterations, as shown in Fig.4.17. It was observed that this temperature, first falls down from conduction temperature and then rises again gradually with number of outer iterations, till it settles down at a constant value below conduction temperature,

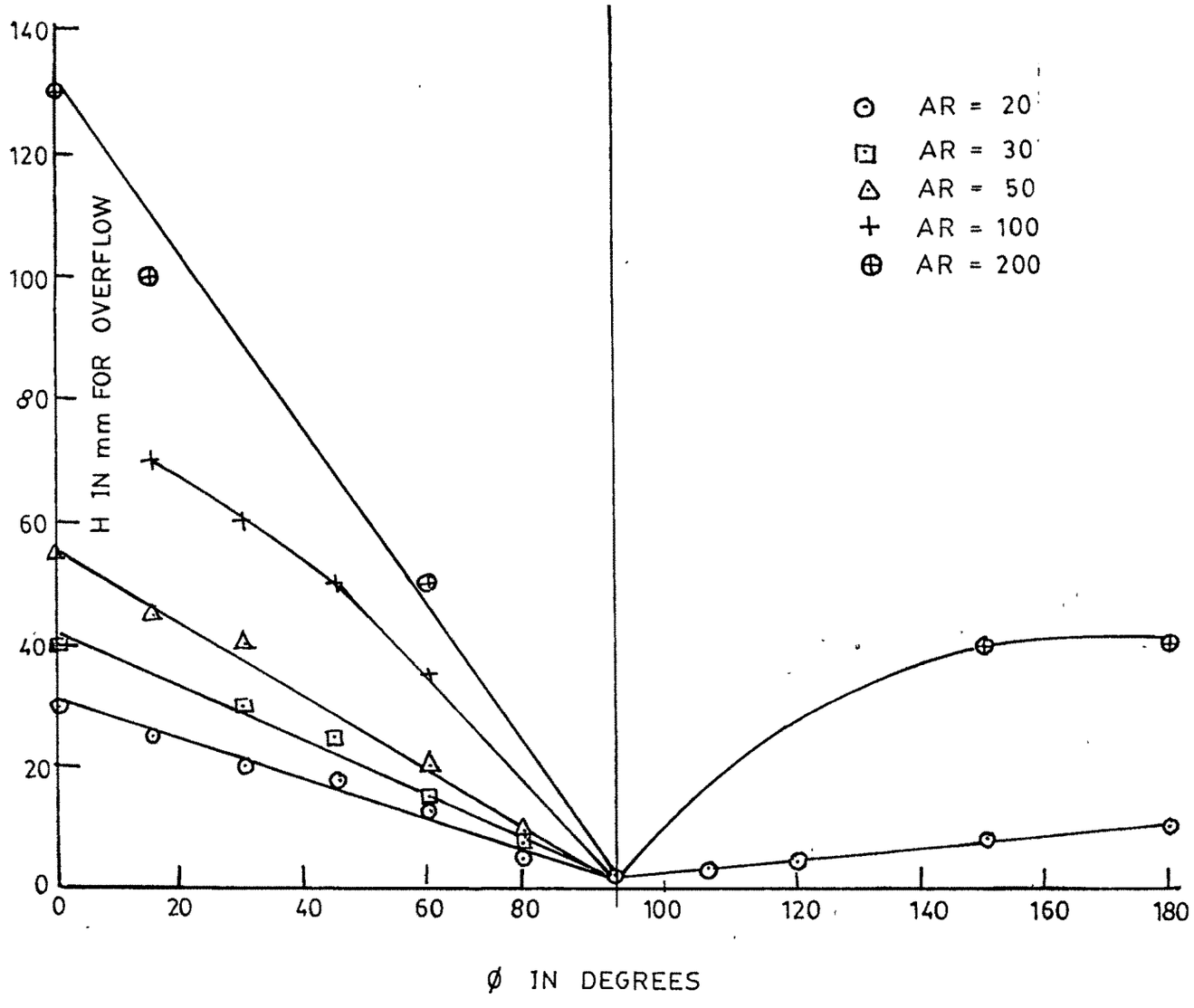
140
120
100
80
60
40
20
0
H IN mm FOR OVERFLOW
AR = 20
AR = 30
AR = 50
AR = 100
AR = 200
0
20
40
60
80
100
120
140
160
180
Ø IN DEGREES

FIG: 4·15

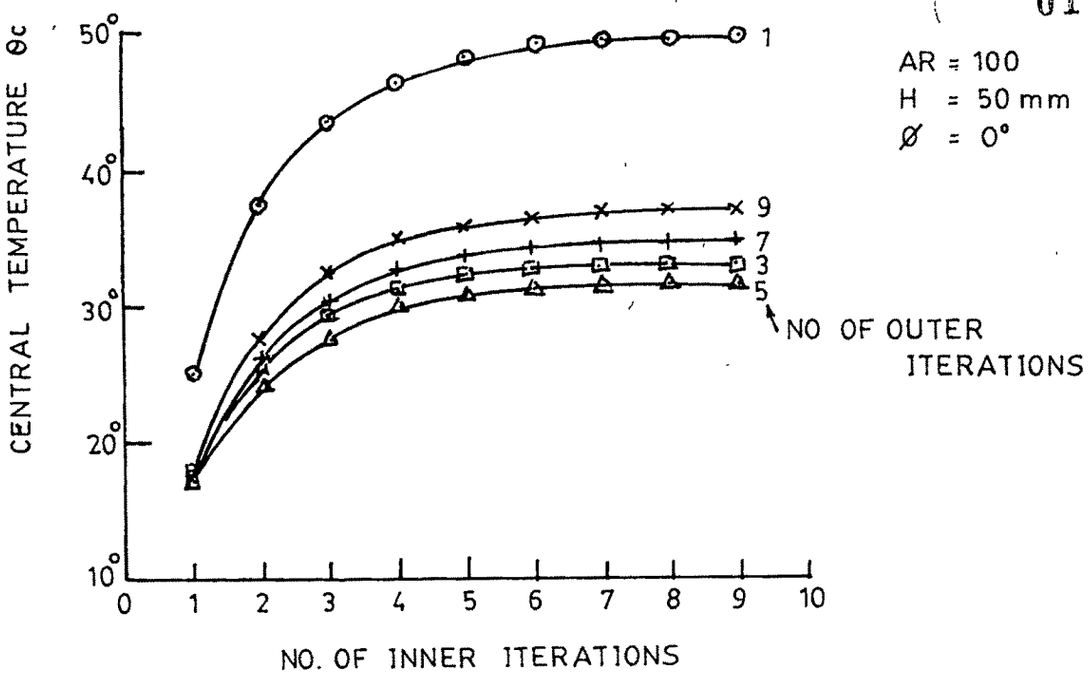

FIG. 4·16

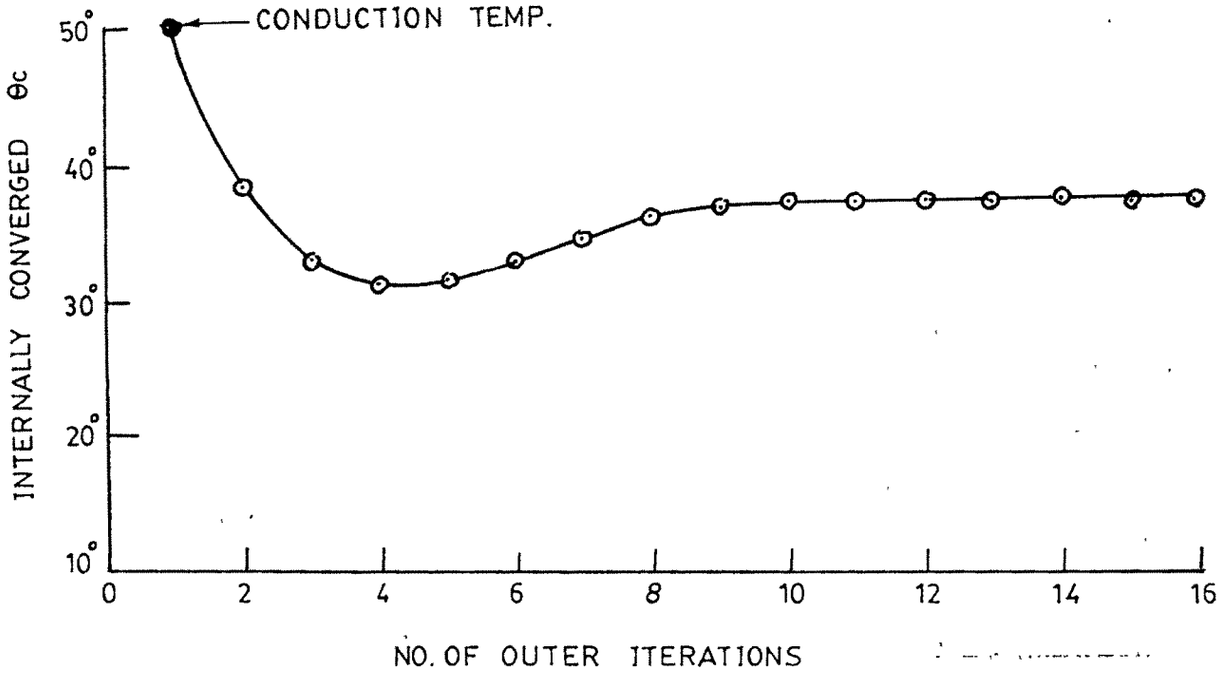

FIG: 4·17

when outer or global convergence occurs. This outer convergence of central temperature depends strictly upon simultaneous outer convergence of stream function and vorticity. This is depicted in Fig.4.18, which shows that, on the same scale, θ_c values are relatively insensitive compared to ψ_c and ω_c values with reference to outer iterations. Heavy fluctuations in central vorticity (ω_c) values during initial outer iterations, proves beyond doubt, the key role played by this function in obtaining a satisfactory solution.

4.3.6 **Effect of Computing Environment :** On the INCONIX system 4000 computer that was used in the present investigation, there was an option of computing in single precision environment or in double precision environment. Thus an experiment was conducted to investigate the effect of computing environment on the results. This is shown in Fig.4.19. It was observed that the errors involved in the results due to single precision (SP) computations were moderate, to within 5% of these obtained by double precision (DP) computations, for moderate values of Rayleigh number, of upto 2.24×10^5 in the test runs for AR=100. However, there was a noticeable increase in the errors at higher Ra values. This observation was complimented by the fact that single precision computations required about 5 minutes for a test run while double precision computations for the same run required about 50 minutes, a ten-fold increase in CPU time.

Thus for reasons of economy of computation and keeping in view the possibility of frequent power supply failure during computation, from operational point of view, it was decided to use single precision environment for computations.

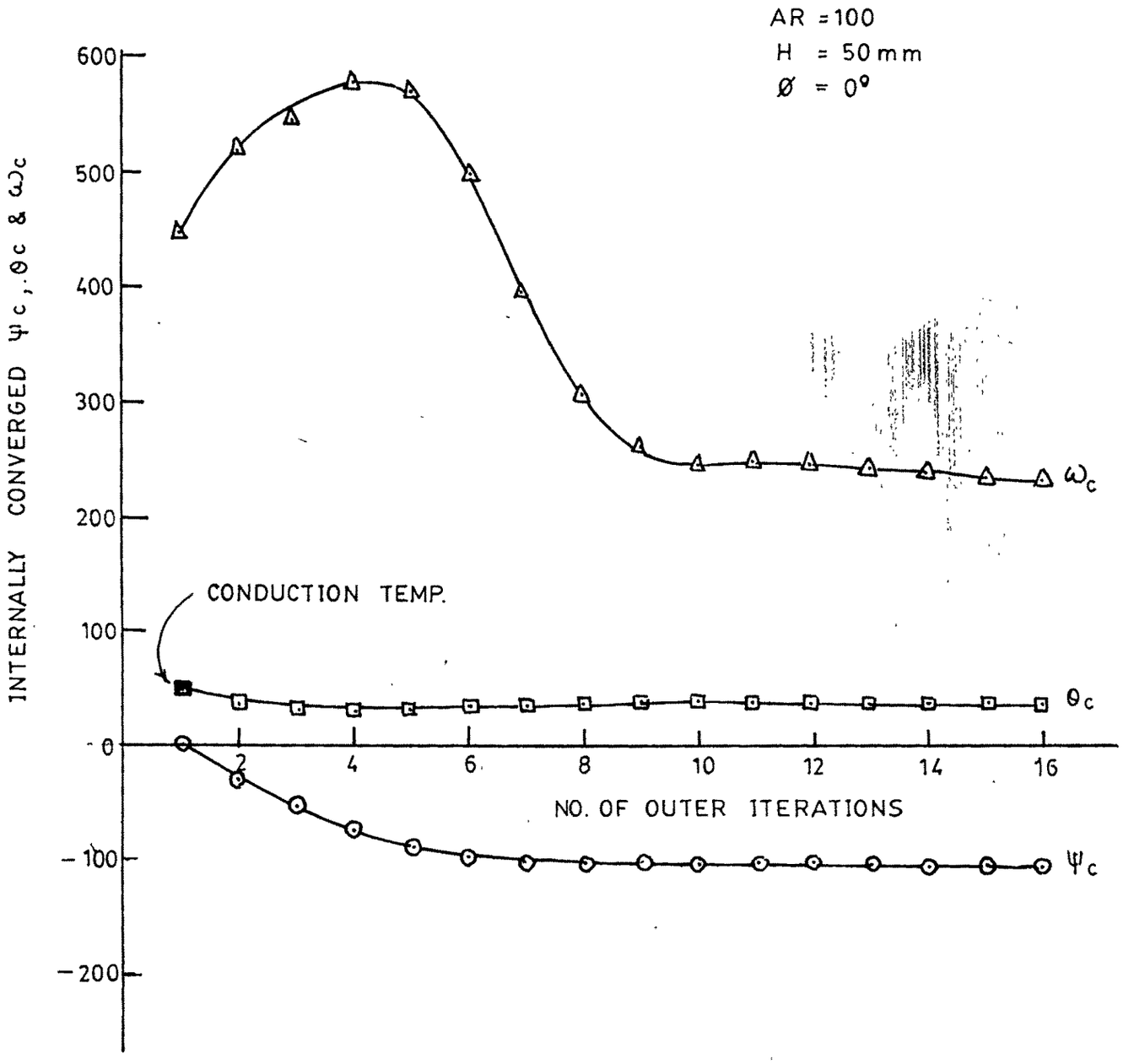
AR = 100
H = 50 mm
Ø = 0°
INTERNALLY CONVERGED Ψc, θc & ωc
600
500
400
300
200
100
0
-100
-200
2
4
6
8
10
12
14
16
NO. OF OUTER ITERATIONS
CONDUCTION TEMP.
ωc
θc
Ψc

FIG: 4·18

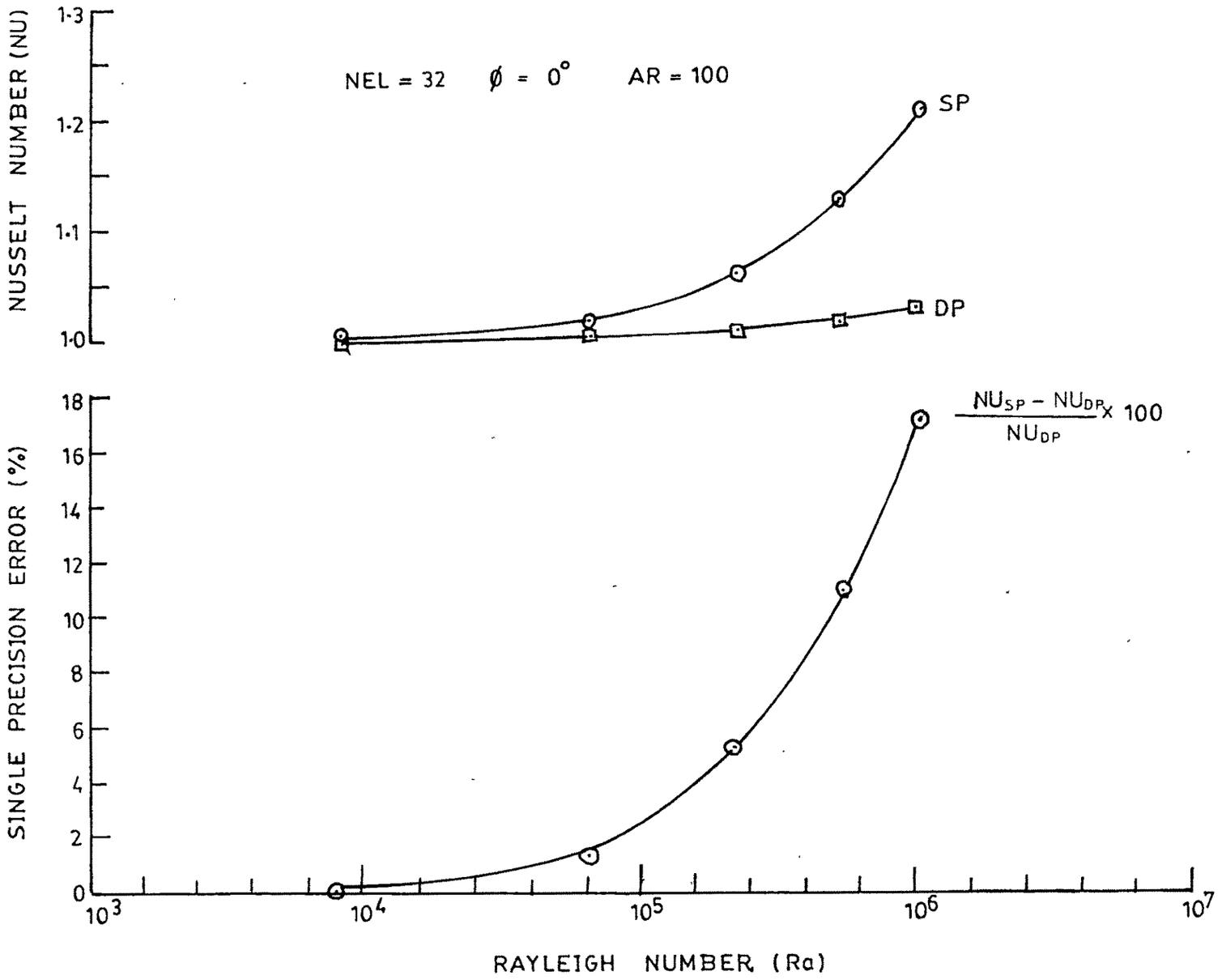
NUSSELT NUMBER (NU)
1·3
1·2
1·1
1·0
NEL = 32 ∅ = 0° AR = 100
SP
DP
SINGLE PRECISION ERROR (%)
18
16
14
12
10
8
6
4
2
0
$\frac{NU_{SP} - NU_{DP}}{NU_{DP}} \times 100$
10^3
10^4
10^5
10^6
10^7
RAYLEIGH NUMBER (Ra)

FIG: 4·19

4.4 COMPUTATIONAL PLAN :

The computer programme in FORTRAN IV developed for the present investigation, was tested for conduction and after getting satisfactory solution in conduction, the programme was run as under :

i) Fixing the aspect ratio of a horizontally oriented enclosure, solutions were obtained at various gap heights i.e. Rayleigh numbers. Similar runs were made for a range of aspect ratios from 1 to 300, while gap height was varied from 2 mm to 160 mm thus varying the Rayleigh number from 66 to 3.4 X 10^7.

ii) Similar solutions were obtained at various enclosure inclinations from 0° to 180° with reference to horizontal.

iii) The output of each run for horizontal enclosures and of representative runs for inclined enclosures was obtained on the printer which included documentation of Nusselt number, gap conductance, Ψ error, θ error, ω error and number of outer iterations, at the time of convergence. It also included stream function, vorticity function and temperature values at all the nodes of the finite element grid.

Present investigation, following the above computational plan, resulted into number of interesting and enlightening observations, which are discussed in the next section.